Applied Catalysis, 71 (1991) 363-391
Elsevier Science Publishers B.V., Amsterdam

Zirconia as a support for catalysts

Influence of additives on the thermal stability of the porous texture of monoclinic zirconia

P.D.L. Mercera*, J.G. van Ommen, E.B.M. Doesburg, A.J. Burggraaf, and J.R.H. Ross

Laboratory of Inorganic Chemistry, Materials Science and Catalysis, Faculty of Chemical Technology, University of Twente, P.O. Box 217, 7500 AE Enschede (Netherlands), tel. (+31-53) 892860, fax. (+31-53) 356024

(Received 5 November 1990, revised manuscript received 28 December 1990)

Abstract

A single-phase monoclinic zirconia (the thermodynamically stable modification up to a temperature of 1170°C), having a specific surface area of 67 m^2g^{-1} and a well-developed mesoporous texture, has been prepared by gel-precipitation followed by calcination at 450°C. A commercially available high-surface area monoclinic zirconia powder ($S_{BET}=71$ m^2g^{-1}) has also been studied. It was found that the specific surface area and pore volume of monoclinic zirconia both decreased markedly on increasing the calcination temperature; despite the fact that the crystal structure was that of the stable modification, this did not seem to impart any substantial resistance to thermal sintering. The thermal stability of monoclinic zirconia could however be improved significantly by addition (by an impregnation technique) of various oxides: CaO, Y_2O_3, La_2O_3 all led to an improvement in the thermal stability up to 900°C while MgO exhibited stabilizing properties only up to 700°C; the best results were obtained with La_2O_3. All the additives investigated other than MgO were found to bring about a partial transition of the monoclinic to a fluorite-like phase of zirconia upon heat treatment; this phase has been shown in the case of the CaO-doped sample to be cubic zirconia and in the cases of the Y_2O_3- and La_2O_3-doped samples to be tetragonal zirconia. As little as 20-50% of a theoretical monolayer quantity of La_2O_3 was sufficient to give satisfactory thermal stability. The results can be explained by a model involving mass transport by a surface diffusion mechanism.

Keywords: zirconia (monoclinic), catalyst preparation (additives), thermal stability, sintering.

INTRODUCTION

Zirconia is currently attracting considerable interest as support material in a variety of catalyst systems [1,2]. In most of the cases, this interest can be ascribed to at least one of the following two properties of zirconia: (i) as a carrier, it gives rise to an unique kind of interaction between the active phase and support, this being manifested in both the catalytic activity and the selec-

0166-9834/91/$03.50

tivity pattern of the system; and (ii) it is more chemically inert than the classical supports (e.g. Al_2O_3 and SiO_2).

Fujii et al. [3] found that zirconia was an excellent support for a $La_{0.8}Sr_{0.2}CoO_3$ catalyst used for the complete oxidation of propane. The use of zirconia as a support gave results which were superior to those obtained with Al_2O_3, SiO_2 or TiO_2, or with the bulk (unsupported) perovskite. Bruce and Mathews [4] and Bruce et al. [5] found that whereas nickel supported on the classical supports gave rise to methanation of $CO + H_2$ mixtures, zirconia-supported nickel had a selectivity which was shifted towards higher hydrocarbons, there being a high proportion of alkenes in the product. Turlier et al. [6], Gavalas et al. [7] and also Smith et al. [8] found that NiO did not interact strongly with ZrO_2 whereas the $NiO–Al_2O_3$ and $NiO–SiO_2$ interactions, for example, were extensive at the interface between the NiO and the supporting oxide; this interaction was particularly marked when relatively high (calcination) temperatures were used. (It should be noted that no compound equivalent to $NiAl_2O_4$ or Ni_2SiO_4 is known for the system NiO/ZrO_2.) Various groups [6–10] have shown that the extent of interaction had a profound effect on the reducibility of the NiO, on the resultant dispersion of the metallic nickel and on the catalytic activity of the reduced catalysts.

For most industrial applications, supports must possess a high accessible specific surface area, good thermal and chemical stabilities, and high mechanical strength. We have previously shown [2] that zirconia with a high specific surface area and a well-developed mesoporous texture can be made by means of gel-precipitation. However, the thermal stability of the predominantly *tetragonal* zirconia samples prepared was not satisfactory: the high specific surface area obtained after calcination at 450 °C ($S_{BET} = 111\ m^2\ g^{-1}$) decreased markedly with increase of temperature (up to 850 °C). Two processes were identified as being responsible for the changes in the pore structure and surface area occurring on calcination in air: (i) crystallite growth and an accompanying phase transformation [from the (metastable) tetragonal into the monoclinic phase]; and (ii) intercrystallite sintering (i.e. agglomeration, neck-formation and growth). It was concluded that the mass-transport mechanism via which the textural changes occurred was surface diffusion.

Monoclinic zirconia is the thermodynamically stable modification at all temperatures below 1170 °C [11]. As our previous work [2] and that of other groups [12–16] have shown that the textural instability of *tetragonal* zirconia is to a great extent associated with the phase transition to the monoclinic modification, we have now carried out a series of experiments aimed at developing a high-surface-area monoclinic zirconia. The preparation of single-phase monoclinic zirconia has been described by a number of investigators. The synthesis routes which have been described include: (i) gel-precipitation of various zirconium salts at a specific pH followed by calcination [14,17–19]; (ii) hydrolytic condensation of zirconium alkoxides followed by calcination [20–22]; (iii)

hydrothermal treatment of amorphous hydrous zirconia employing different mineralizers [23,24]; (iv) flame hydrolysis of zirconium chloride [13,25]; and (v) refluxing of either $ZrOCl_2$-solutions or amorphous hydrous zirconia in different media [12,26–28]. However, all these preparation techniques were reported to yield monoclinic zirconia which either had a relatively low specific surface area or was highly microporous. (The preparation method used by Bensitel et al. [22] was reported to yield a non-microporous monoclinic zirconia powder with a specific surface area of 81 $m^2 g^{-1}$ after calcination at 447 °C; however, very few details were given concerning the preparation conditions.) As our aim is to develop high-surface-area zirconia without any microporosity, alternative ways of preparing single-phase monoclinic zirconia samples have been developed in our laboratory. This paper thus describes: (i) a synthesis route to give high-surface-area single-phase monoclinic zirconia; (ii) the results of a systematic study of the stability of the porous texture of monoclinic zirconia after calcination in static air at various temperatures up to 900 °C; and (iii) the influence of different additives on the sintering of a commercial monoclinic zirconia sample.

EXPERIMENTAL

Preparation of single-phase monoclinic zirconia

Single-phase monoclinic zirconia samples were made by a slight modification of the gel-precipitation technique which was described previously [2]; the most important difference involved subjecting the Cl^--free hydrogel to two extra cycles of redispersion in ethanol. Work done in our laboratory showed that ethanol-washing, besides having the well-documented influence on the morphology of the resultant powders [29–32], had an influence on the evolution and stability of the different crystal modifications of zirconia. Ethanol-washing was in fact found to strongly promote the (metastable) tetragonal-to-monoclinic phase transformation. Full details regarding the interaction of ethanol with (hydrous) zirconia will be given elsewhere [33].

Precipitation was carried out at room temperature at a constant pH of 10.0 by the simultaneous addition of a solution of zirconyl chloride (Merck, Pro Analysis, 0.4 *M*) and another of ammonia (Merck, Pro Analysis, 6.7 *M*) to doubly distilled water (the pH of which had previously been adjusted to 10.0 with ammonia). The precipitate formed was aged in the mother liquor for 65 h, after which it was filtered and then washed in a sequence of repeated cycles involving redispersion in doubly distilled water and filtration. The water-washing steps were continued until a negative test for chloride ions was obtained ($AgNO_3$-test, 3 *M* $AgNO_3$ solution). The Cl^--free hydrogel was then subjected to two cycles involving redispersion in ethanol (purity 99.8%) followed by filtration. The precipitation and washing steps were carried out in

the reactor described previously [2,34]. After the final dispersion/filtration step, the hydrous zirconia was dried in air at 110°C for 20 h and then dry-milled in a plastic container employing teflon balls. The X-ray amorphous powder thus obtained was calcined at 450°C for 15 h in static air (heating rate: 3°C min^{-1}; cooling rate: 2°C min^{-1}) and this resulted in a well-crystallized monoclinic zirconia powder. The sample prepared in this way was termed ZC5-10E.

A commercially available high-surface-area monoclinic zirconia powder, RC100, supplied by Daiichi Kigenso Kagaku Kogyo (Japan), was also used in the present study. As will be shown in the next section, this powder is comparable, both in purity and properties, with the monoclinic zirconia sample made in our laboratory.

Preparation of the doped zirconium oxides

The influence of various additives on the sintering behaviour of monoclinic zirconia was studied using the commercial powder RC100 as the starting/reference material. The additives investigated were MgO, CaO, Y_2O_3 and La_2O_3. These particular oxides were selected according to the following criteria: (i) the effective cationic radius of the dopant must be similar to or larger than that of the zirconium ion to minimize the chance of solid-solution formation with monoclinic zirconia and to influence the mass transport mechanism involved in the sintering of this material; and (ii), the valency of the cation must be invariant to avoid secondary effects arising from oxidation or reduction of the dopant. The effective cationic radii of the additives investigated and their coordination numbers are compared with those of the zirconium ion in Table 1 (these data were taken from ref. 35). Assuming that surface diffusion is the

TABLE 1

Effective cationic radii of the additives investigated

Oxide	Cationic coordination number	Effective cationic radius (Å)
ZrO_2	7	0.78
	8	0.84
MgO	6	0.72
	8	0.89
CaO	6	1.00
	8	1.12
Y_2O_3	6	0.90
	8	1.02
La_2O_3	6	1.03
	8	1.16

predominant mass transport mechanism, we chose to use impregnation of the starting material (RC100) for the addition of the dopants.

A large batch of the as-received RC100 powder was calcined at 400 °C to provide the starting material for impregnation; the calcination was carried out in static air (for 15 h), the heating rate being 3 °C min^{-1} and the cooling rate 2 °C min^{-1}. The relevant physical properties of the resultant powder are collected in Table 2. Aqueous solutions of the corresponding nitrate salts were used for impregnation (Merck, Pro Analysis quality); 25 g of the calcined RC100 powder was dispersed at room temperature in 50 cm^3 of a solution containing the additive in the desired concentration. The suspension was stirred for 3 h, after which the solid was filtered and then dried for 20 h at 90 °C in static air. The dried material was ball-milled in a plastic container using teflon balls and then, after heating at a rate of 0.5 °C min^{-1}, it was calcined in a flow of air (300 cm^3 min^{-1}) at 400 °C for 15 h; the isothermal stage was followed by cooling to room temperature at a rate of 2 °C min^{-1}. The samples thus prepared were designated RC100-αX, where X stands for the additive in question (Mg, Ca, Y,or La) and α for the additive content expressed as a mole percentage (mol-%).

To study possible effects of non-homogeneity of the additive on the sintering behaviour of monoclinic zirconia, some impregnation experiments were carried out using a solution of the complex formed between La^{3+} and EDTA (ethylene diamine tetra-acetic acid); work from Meima [36] and Tijburg [37] has shown that impregnation with 'poorly crystallizing' organometallic complexes (citrates, formates and EDTA-complexes) results in homogeneous distribution of the impregnated component. The $[La(EDTA)]^-$ impregnation solutions were prepared according to the procedure described by Tijburg [37]. The desired amount of $La(NO_3)_3 \cdot 6H_2O$ (Merck, Pro Analysis) was dissolved in 15 cm^3 of doubly distilled water. An equimolar amount of EDTA (Merck, Pro Analysis) was dissolved in 20 cm^3 doubly distilled water by raising the pH to

TABLE 2

Physical properties of the RC100 powder used in the impregnation experiments

Crystallographic phase	$S_{BET}{}^{\alpha}$ (m^2 g^{-1})	$S_t{}^{\beta}$ (m^2 g^{-1})	$V_p[0.95]^{\gamma}$ (cm^3 g^{-1})	$R_p(ads)^{\delta}$ (Å)	$R_p(des)^{\epsilon}$ (Å)
99% monoclinic	71	72	0.18	41	33

[α]Specific surface area calculated according to the BET method.

[β]Surface area calculated using the *t*-plot method.

[γ]Specific pore volume calculated from adsorption at $p/p^0 = 0.95$.

[δ]Most frequent pore radius calculated from the adsorption data, employing the BJH method and assuming cylindrical pore model.

[ε]Most frequent pore radius calculated from the desorption data.

a value between 5 and 6 by addition of a 25% ammonia solution (Merck, Pro Analysis). The $La(NO_3)_3$-solution was slowly added to the EDTA-solution, the pH being maintained at a value between 5 and 6 by the addition of concentrated ammonia. Finally, the volume of the solution was raised to the required 50 cm^3. The impregnation of the RC100 powder and the drying and calcining were then carried out following the procedure described above. The samples prepared in this way were designated RC100-αLaE; α has the same significance as above.

Chemical analysis

The purity of ZC5-10E and RC100, and the quantities of CaO, Y_2O_3 and La_2O_3 introduced were determined using X-ray fluorescence analysis (XRF, Philips PW 1410 spectrometer). The amount of MgO introduced was determined by means of atomic absorption spectroscopy (AAS).

Sintering experiments

The sintering studies were performed by calcining the samples at various temperatures up to 900 °C. Calcination was carried out in static air in a Stanton Redcroft tube furnace. The temperature was increased at a rate of 3 °C min^{-1} to the final temperature; this was maintained for 15 h before the sample was cooled to 200 °C at a rate of 5 °C min^{-1} and then cooled rapidly to room temperature.

Characterization techniques

The calcined samples were characterized by nitrogen physisorption measurements, Raman spectroscopy, transmission electron microscopy (TEM) and X-ray powder diffraction (XRD). Full nitrogen adsorption/desorption isotherms at −196 °C were obtained using a Micromeritics ASAP 2400 system. Prior to the physisorption measurements, all the samples were outgassed for 6 h at 300 °C. Analysis of the isotherms was carried out as described previously [2]. Raman spectra of selected samples were obtained with a SPEX 1877 spectrometer equipped with an Ar^+-ion laser (wave length, $\lambda = 514.5$ nm and power $W = 20$–25 mW).

Transmission electron microscopy was carried out using a JEOL 200CX electron microscope operated at 200 kV. TEM specimens were prepared by ultrasonically dispersing the powder samples in ethanol (Merck, Pro Analysis) and then applying drops of this suspension to a holey carbon film supported on a copper grid.

X-ray diffraction patterns were recorded using a Philips PW 1710 diffractometer with Ni-filtered Cu Kα radiation. Both continuous and step-scan

techniques were used, the latter being employed for quantitative analysis. The step-scans were taken over the range of 2θ from 26 to 33° in steps of 0.015° (2θ), the intensity data for each point being collected for 10 s. In order to further improve counting statistics, rotation about the normal axis was used. The collected data were analysed according to the procedure described previously [2]; this involved resolving the overlapping peaks by best-fitting the diffraction profiles using asymmetric Lorentzians.

The volume fraction (V_m) of the monoclinic phase in the samples was estimated from the integrated intensity ratio X_m (eqn. 1):

$$X_m = \frac{I_m(11-1) + I_m(111)}{I_m(11-1) + I_m(111) + I_f(111)} \quad (1)$$

using the non-linear relationship (eqn. 2) proposed by Toraya et al. [38]:

$$V_m = \frac{1.31\, X_m}{1 + 0.31\, X_m} \quad (2)$$

The subscripts m and f represent the monoclinic and the 'fluorite-like' phases (either tetragonal or cubic), respectively.

The crystallite sizes (D_{hkl}) of selected samples were calculated from the pattern-resolved peaks for the (11−1) and (111) reflections of the monoclinic phase and for the (111) reflection of the fluorite-like phase by using the Scherrer relationship (eqn. 3):

$$D_{hkl} = \frac{0.9\lambda}{B_{hkl}\cos\theta} \quad (3)$$

B_{hkl}, the width of the peak at half the peak maximum corrected for both the effect of spectral and instrumental broadening, was determined as described previously [2].

RESULTS

Undoped monoclinic zirconia

XRF analyses showed that the samples ZC5-10E and RC100 were high-purity zirconium oxides (> 99.8%), the major contaminant in both samples being hafnium. Traces of the following impurities were detected: titanium, iron and silicon, the RC100 powder was also found to contain traces of aluminium and sodium. XRD confirmed that ZC5-10E and RC100, calcined at 450°C and 400°C, respectively, were almost pure monoclinic zirconium oxides; the volume fraction (V_m) of the monoclinic phase was calculated to be 0.90 for ZC5-10E and 0.99 for RC100. The small fraction of the tetragonal phase present

was progressively converted into the monoclinic modification on increasing the calcination temperature; both samples were 100% monoclinic after heat treatment at temperatures above about 550 °C. (Note that in a previous publication [2], we reported on the phase evolution upon heat treatment of zirconia samples which were subjected to the *water-washing steps only* and showed that calcination in flowing air at, for example, 450 °C for 15 h yielded a powder which contained more than 70% tetragonal zirconia).

The effect of thermal treatment on the evolution of the specific surface area (S_{BET} and S_t) and specific pore volume ($V_p[0.95]$) of the monoclinic samples ZC5-10E and RC100 are shown in Figs. 1a and b respectively. The values of S_{BET} were calculated by the BET-method, assuming a value of 0.162 nm^2 for the cross-sectional area of the nitrogen molecule [39,40]; the values of S_t, the sum of the areas of the mesopore walls and the external surface, were determined using the *t*-plot method [41]. The values of the pore volume, V_p [0.95], were calculated from adsorption at $p/p^0 = 0.95$ by assuming the Gurvitsch rule [39]. From the Figs. 1a and b, it is clear that, notwithstanding the fact that both the samples are structurally stable, the porous texture of the zirconium oxides investigated is not stable under the experimental conditions employed, even at the lower calcination temperatures: the initially high specific surface area and pore volume decrease markedly on increasing the calcination temperature. Fig. 1a shows also that the two single-phase monoclinic samples have

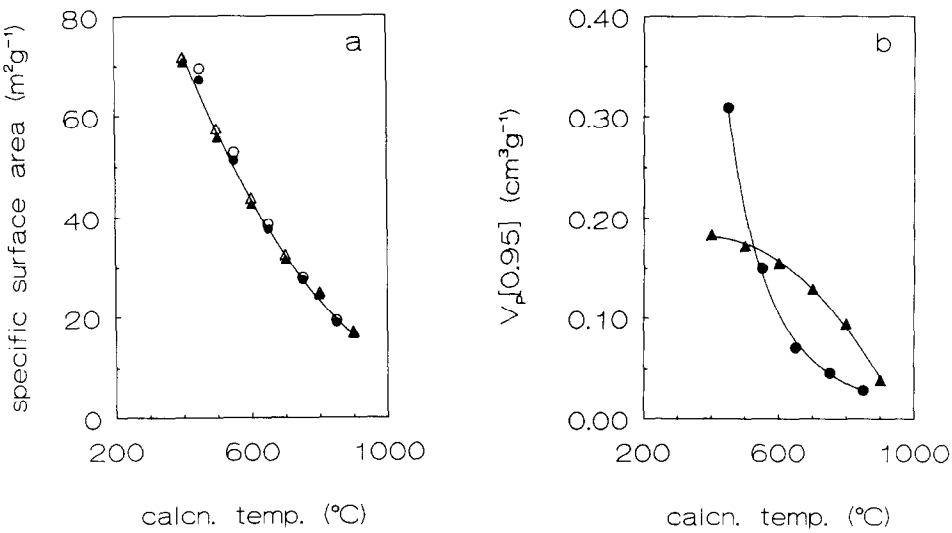

Fig. 1. The effect of calcination temperature on the textural characteristics of an undoped single-phase monoclinic zirconia samples ZC5-10E (● and ○) and RC100 (▲ and △). (a) Closed symbols, BET specific surface area (S_{BET}); open symbols, specific surface areas from *t*-plots (S_t). (b) Specific pore volume calculated from adsorption of nitrogen at $p/p^0 = 0.95$ ($V_p[0.95]$).

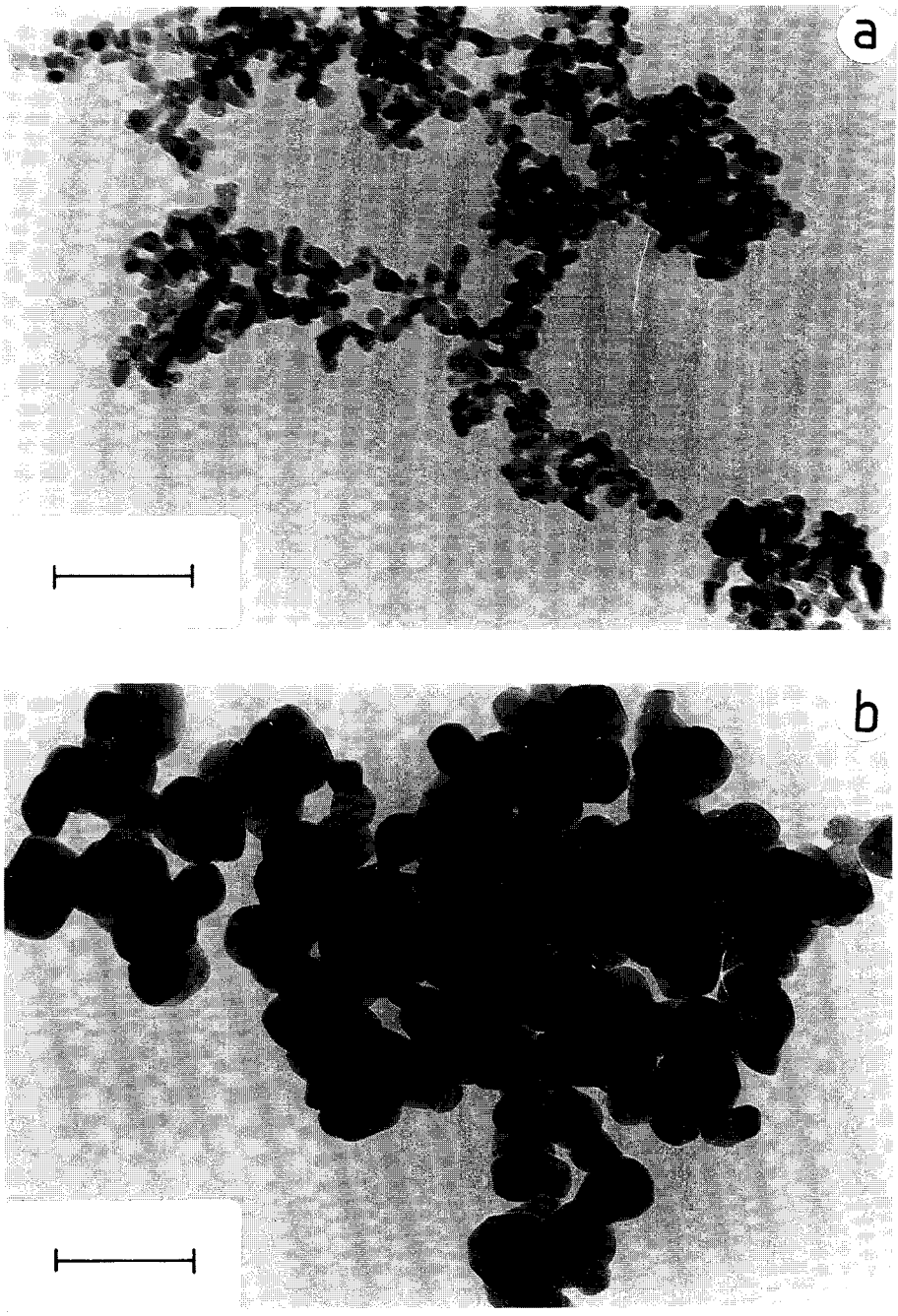

Fig. 2. Transmission electron micrographs of ZC5-10E, calcined at (a) 450 °C and (b) 850 °C, and of RC100, calcined at (c) 500 °C, (d) 700 °C and (e) 900 °C. The bar indicates a measurement of 100 nm.

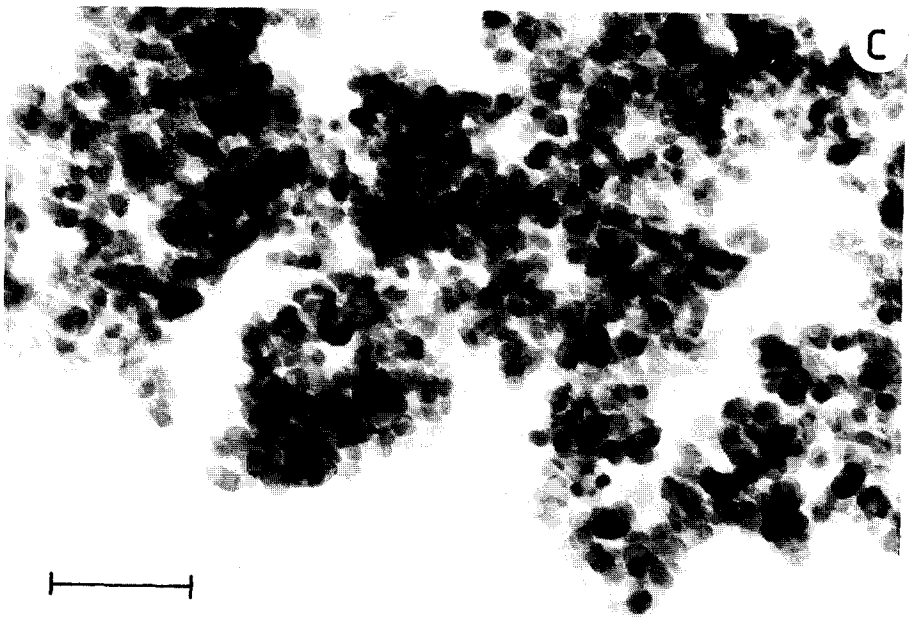
c

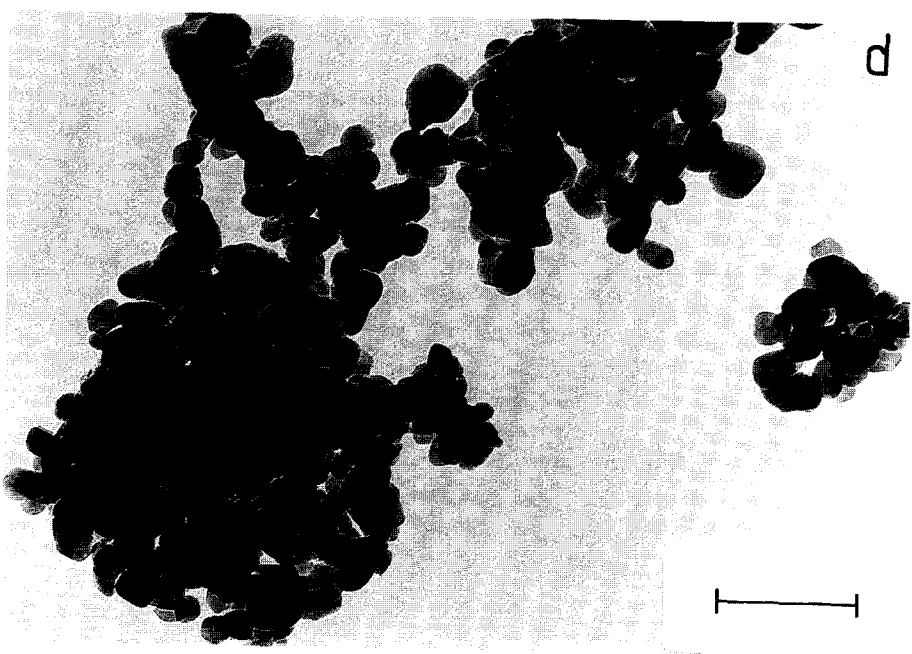
d

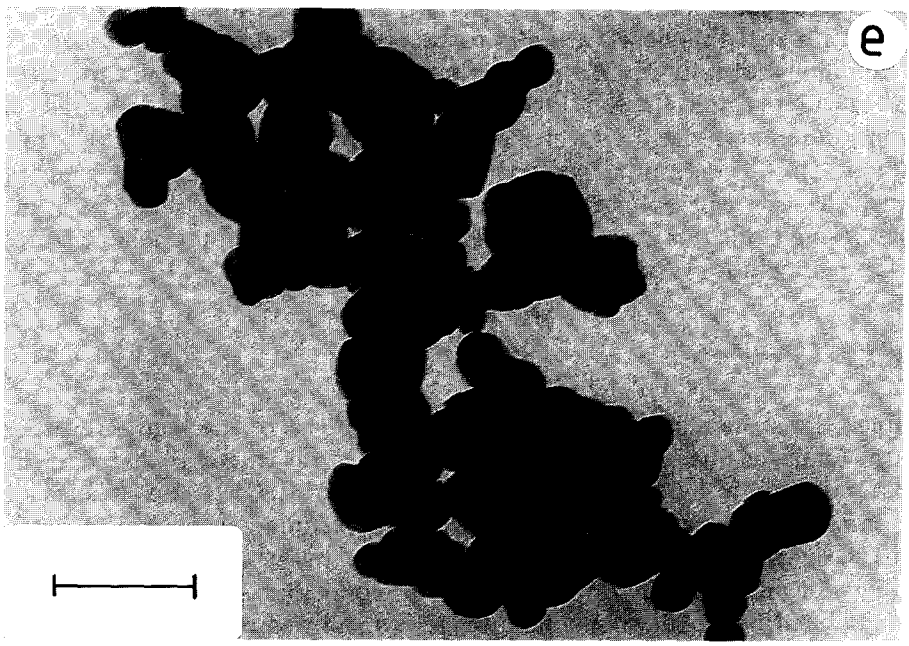

similar specific surface areas at all calcination temperatures. Furthermore, it can be inferred from this figure that the surface area of these samples is located within their meso- and macropores; the S_{BET}-values are in close agreement with the calculated S_t-values and this is indicative of the absence of microporosity [2,39]. The variation with calcination temperature of the specific pore volume ($V_p[0.95]$) is different for the two samples (Fig. 1b). Not only is the initial specific pore volume of ZC5-10E larger than that of RC100 but it also decreases more markedly with increasing calcination temperature than does the specific pore volume of RC100. (Results not reported in detail here showed that the values of the initial specific pore volumes of samples analogous to ZC5-10E depended on the conditions and method used for drying as well as on the calcination atmosphere.)

TEM and X-ray line broadening analyses showed that the monoclinic crystallites of ZC5-10E and RC100 increased drastically in size upon heat treatment. To give an impression of the extent of this crystallite growth process, representative TEM micrographs of selected calcined samples are presented in Fig. 2; the micrographs 2a and b show the results for the sample ZC5-10E calcined at 450 and 850°C, respectively, and the micrographs 2c–e show the results for the samples RC100 calcined at 500, 700 and 900°C, respectively. All the micrographs are shown at the same magnification. (Note that the morphology of ZC5-10E calcined at 450°C (micrograph 2a) appears to be much

more 'open' and much less agglomerated than that of RC100 calcined at 500 °C (micrograph 2c); this observation is in good agreement with the respective pore volumes shown in Fig. 1b.) The values of the monoclinic crystallite sizes (D_{hkl}) calculated from the XRD results for the RC100 powder as a function of calcination temperature are given in Fig. 3; the values are in excellent agreement with the TEM results. Fig. 3 also shows that there is a good agreement between the sizes calculated from the (11–1) and (111) reflections. This particular result is also in accordance with the TEM results and demonstrates that the monoclinic crystallites are isometric in shape.

Influence of additives

Table 3 lists the additives investigated in this part of the study, together with the analysed quantities of the additives; the latter values are listed as the mole fractions of MgO, CaO, $YO_{1.5}$, and $LaO_{1.5}$ in the ZrO_2. Table 3 also gives the number of cations calculated per surface Zr^{4+} ion, i.e. the amount of additive relative to a theoretical monolayer coverage; these values were calculated using a value of $7.30 \cdot 10^{18}$ Zr^{4+} ions per m^2 of monoclinic surface. (This value was calculated using the monoclinic lattice constants given by McCullough and Trueblood [42], assuming that the surface is formed from equal proportions of the (11–1) and (111) planes; it is in good agreement with the monolayer capacity established experimentally by Pratt et al. [43].) It can be seen

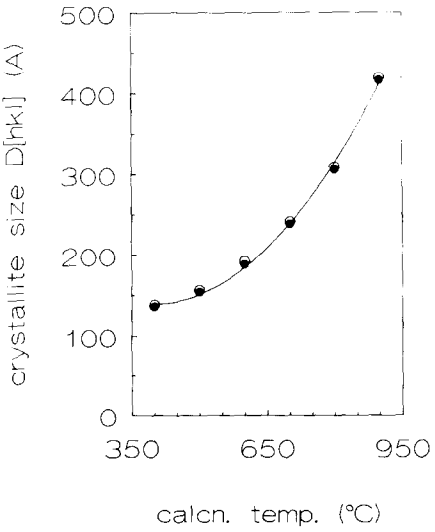

Fig. 3. Effect of calcination temperature on the process of crystallite growth in RC100; (●) the size calculated using the (11 – 1) reflection of the monoclinic phase; (○) the size calculated using the (111) reflection of the monoclinic phase.

TABLE 3

Additives investigated and their analysed content

Code	Additive	Mole fraction additive[α]	Number of cations calculated per surface Zr^{4+} ion
RC100-5.2Mg	MgO	0.052	0.52
RC100-5.8Ca	CaO	0.058	0.58
RC100-5.4Y	$YO_{1.5}$	0.054	0.54
RC100-5.4La	$LaO_{1.5}$	0.054	0.54

[α]Mole fraction of additive defined by $n_M/(n_M+n_{Zr})$, n_i being the amount of cation i in mol.

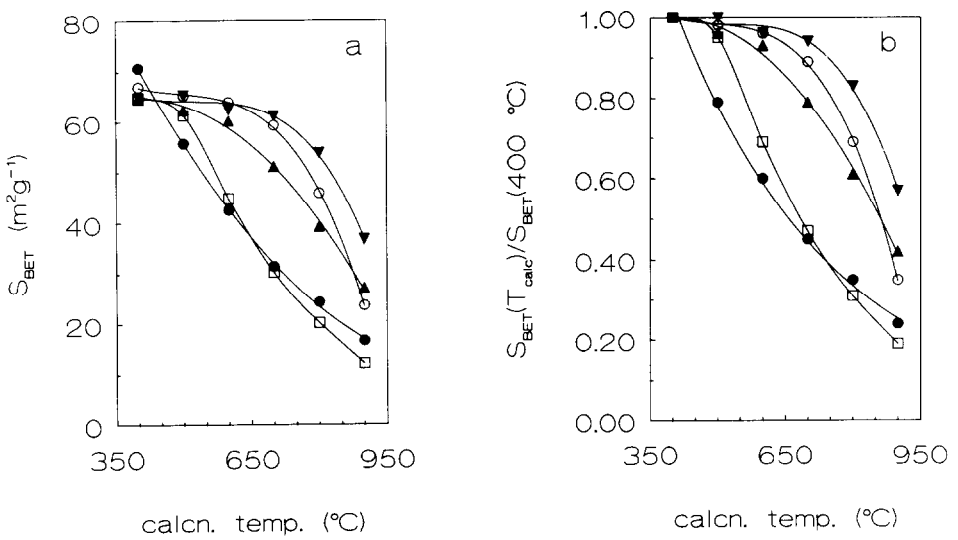

Fig. 4. The influence of various additives on the thermal stability of 'monoclinic' zirconia. (a) The variation of the BET specific surface area with calcination temperature; (b) the relative thermal stability expressed as the fraction of the initial BET area which is retained after sintering. (●) Undoped monoclinic sample (RC100); (□) the sample doped with 5.2 mol-% MgO (RC100-5.2Mg); (▲) the sample doped with 5.8 mol-% CaO (RC100-5.8Ca); (○) the sample doped with 5.4 mol-% $YO_{1.5}$ (RC100-5.4Y); and (▼) the sample doped with 5.4 mol-% $LaO_{1.5}$ (RC100-5.4La).

that the additive concentrations investigated in this part of the study are equivalent to approximately half of the theoretical monolayer. Analysis of the X-ray diffractograms of the doped samples showed that there were no discernible reflections other than those of zirconia itself after calcination at 400 or 500°C. This implies that the additives were initially present in highly dispersed or amorphous states.

The results of the sinter experiments in static air are presented in Figs. 4a and b. These show that all the additives investigated other than MgO improve

the thermal stability of monoclinic zirconia over the entire range of temperatures studied, *La_2O_3 being the most effective*. MgO reduces the loss of surface area only at calcination temperatures up to 700°C; above this temperature, MgO is seen to have a detrimental effect on the surface area of monoclinic zirconia. It should be noted that the small differences in the specific surface areas for the materials calcined at 400°C (Fig. 4a) are due to either pore filling (MgO or CaO) or to the large added mass of the additive (Y_2O_3 or La_2O_3) (see also the next subsection).

Phase-analyses employing XRD showed that CaO and Y_2O_3, and to a much lesser extent also La_2O_3, brought about a transition of the monoclinic to a fluorite-like phase of zirconia upon sintering; using XRD supplemented by Raman spectroscopy, this phase was shown to be cubic zirconia in the case of the CaO-doped sample and tetragonal zirconia in the cases of the Y_2O_3- and La_2O_3-doped samples. X-ray reflections due to free CaO, Y_2O_3 or La_2O_3 were not observed. However, the diffractogram of the La_2O_3-doped sample calcined at 900°C provided evidence for the formation of the pyrochlore compound $Zr_2La_2O_7$. On the other hand, the X-ray diffractograms of the MgO-doped samples showed no discernable reflections pertaining to a fluorite-like phase. In fact, only reflections due to the monoclinic phase of zirconia were observed up to 800°C; in the diffractogram of the sample calcined at 900°C, the most intense reflection due to the (200) plane of cubic MgO was detected as well. The results for the phase transition to the stabilized fluorite-like phase of zirconia are shown in Fig. 5; the volume fraction V_m of the (remaining) monoclinic phase is plotted against calcination temperature, the complementary phase being the fluorite-like phase.

Lanthana promoted monoclinic zirconia

Since lanthanum oxide was found to be the most effective stabilizing additive, we concentrated our attention on this oxide. Table 4 lists the various samples prepared together with their analysed lanthana contents. It is clear from this table that the lanthana concentrations investigated are all less than those required for a saturated monolayer. XRD analysis of all the samples after calcination at 400 or 500°C showed no discernible reflections other than those of monoclinic zirconia; this implies that the lanthanum, most probably in the form of an oxide or oxide-carbonate, was initially present in a highly dispersed or amorphous state.

The results of the experiments to examine the effect of the various La_2O_3-concentrations on the BET surface areas after calcination at various temperatures are presented in Fig. 6a; Fig. 6b gives the relative areas after sintering ($S_{BET}(T_{calcn.})/S_{BET}(400°C)$) as a function of the lanthana content for the different calcination temperatures. It is clear that for calcination temperatures in excess of 400°C the thermal stability of monoclinic zirconia is improved to

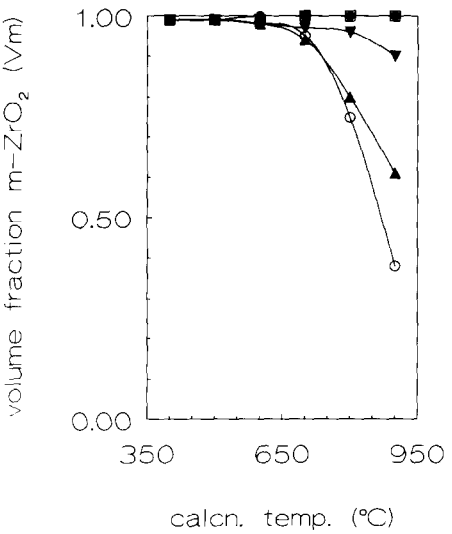

Fig. 5. The influence of various additives on the phase stability of monoclinic zirconia. (●) Undoped (monoclinic) sample (RC100); (□) the sample doped with 5.2 mol-% MgO (RC100-5.2Mg); (▲) the sample doped with 5.8 mol-% CaO (RC100-5.8Ca); (○) the sample doped with 5.4 mol-% $YO_{1.5}$; and (▼) the sample doped with 5.4 mol-% $LaO_{1.5}$ (RC100-5.4La).

TABLE 4

Lanthanum oxide content of the La_2O_3-doped zirconium oxides

Code	Additive	Mole fraction lanthanum[α]	Number of cations calculated per surface Zr^{4+} ion
RC100-2.5La	$LaO_{1.5}$	0.025	0.24
RC100-4.5La	$LaO_{1.5}$	0.045	0.45
RC100-5.4La	$LaO_{1.5}$	0.054	0.54
RC100-6.3La	$LaO_{1.5}$	0.063	0.63
RC100-8.0La	$LaO_{1.5}$	0.080	0.82
RC100-2.7LaE	$LaO_{1.5}$	0.027	0.27
RC100-5.3LaE	$LaO_{1.5}$	0.053	0.52

[α]Mole fraction of lanthanum defined by $n_{La}/(n_{La}+n_{Zr})$, n_i being the amount of cation i in mol.

a considerable extent by the addition of lanthanum oxide (Fig. 6a). After calcination at 400°C, the BET specific surface area (i.e. per gram of promoted oxide) was found to decrease gradually on increasing the lanthanum oxide content; the BET-area decreased from 71 $m^2\ g^{-1}$ for the undoped sample to 58.3 $m^2\ g^{-1}$ for the sample doped with 8 mol.-% $LaO_{1.5}$. There are two possible explanations for this phenomenon: (i) the decrease is a consequence of the (large) added mass of the lanthana; or (ii) the decrease is due to filling of the

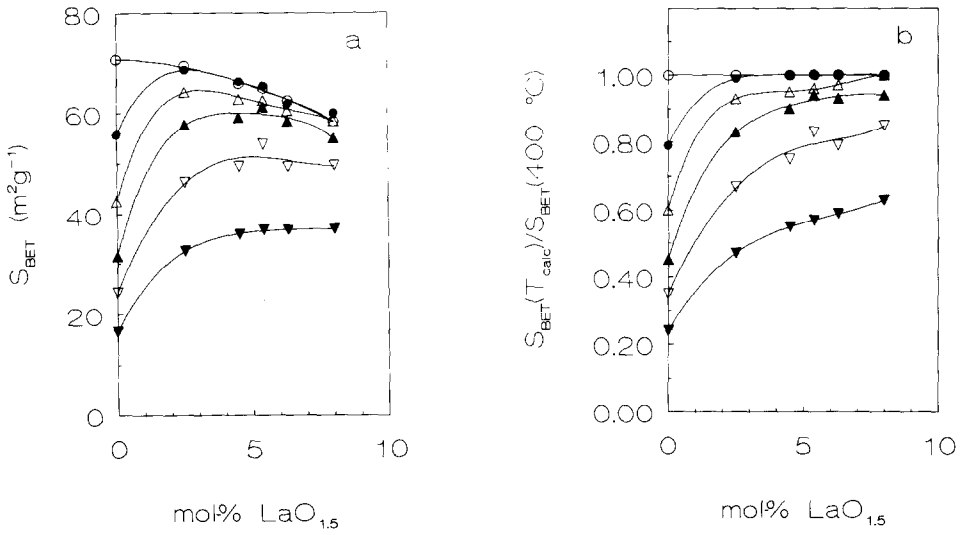

Fig. 6. The influence of lanthanum oxide on the thermal stability of 'monoclinic' zirconia. (a) the variation of the BET specific surface area with $LaO_{1.5}$ concentration after calcination. (b) the effect of $LaO_{1.5}$ concentration on the (relative) retention of the initial BET area, i.e. the relative thermal stability, after sintering. (○) 400°C; (●) 500°C; (△) 600°C; (▲) 700°C; (▽) 800°C; and (▼) 900°C.

TABLE 5

Influence of the impregnation procedure on the textural stability of monoclinic zirconia

$T_{calc.}$ (°C)	RC 100-2.5 La		RC 100-2.7 La	
	S_{BET} ($m^2 g^{-1}$)	S_{BET}/S_{BET} (400°C)	S_{BET} ($m^2 g^{-1}$)	S_{BET}/S_{BET} (400°C)
400	69.4	1	69.4	1
500	68.6	0.99	67.8	0.98
600	64.2	0.93	64.2	0.93
700	57.7	0.83	59.9	0.86
800	46.4	0.67	48.8	0.70
900	32.6	0.47	35.1	0.51

(smallest) pores with lanthanum oxide [44–46]. Recalculation of the initial areas per gram of zirconia showed that the decrease in BET-area was mainly due to the added mass of the lanthana for samples with up to 5.4 mol-% $LaO_{1.5}$; filling of the pores became appreciable at concentrations in excess of 5.4 mol-% $LaO_{1.5}$. When the results are corrected for this initial loss of surface area, it can be seen (Fig. 6b) that the thermal stability improves gradually with increasing lanthanum oxide content; over the range of promoter concentrations studied, particularly at calcination temperatures above 700°C, no plateau was

TABLE 6

Influence of the impregnation procedure on the textural stability of monoclinic zirconia

$T_{calc.}$ (°C)	RC100-5.4La		RC100-5.3LaE	
	S_{BET} ($m^2 g^{-1}$)	S_{BET}/S_{BET} (400°C)	S_{BET} ($m^2 g^{-1}$)	S_{BET}/S_{BET} (400°C)
400	64.9	1	67.4	1
500	65.4	1.01	67.0	0.99
600	62.5	0.96	62.9	0.93
700	61.2	0.94	59.3	0.88
800	53.8	0.83	53.5	0.79
900	36.8	0.57	38.5	0.57

reached. However, for practical applications (e.g. monoclinic zirconia as a catalyst support), promotion with an amount equivalent to 20–50% of the (theoretical) monolayer quantity of $LaO_{1.5}$ is probably enough to ensure that a monoclinic material of a sufficiently high thermal stability is obtained.

The plot of the volume fraction V_m of the (remaining) monoclinic phase versus calcination temperature given in Fig. 5 for the zirconia samples modified with 5.4 mol-% $LaO_{1.5}$ (RC100-5.4La) discussed above is typical of those obtained for the samples promoted with different amounts of $LaO_{1.5}$; all the samples showed a limited transformation to the stabilized tetragonal modification, the volume fraction of which amounted at most to 0.12 for RC100-8.0La after calcination at 900°C. Furthermore, no X-ray reflections due to free La_2O_3 were observed, even for the samples modified with 8.0 mol-% $LaO_{1.5}$. On the other hand, the pyrochlore compound $Zr_2La_2O_7$ was detected for all the samples modified with more than 2.7 mol-% $LaO_{1.5}$; the formation of this compound started above about 700°C.

Tables 5 and 6 give data which show that there is no significant influence of the impregnation procedure/technique on the sintering behaviour of monoclinic zirconia; practically identical results were obtained whether impregnation was carried out with aqueous solutions of $[La(EDTA)]^-$ or of $La(NO_3)_3$.

DISCUSSION

Sintering of undoped single-phase monoclinic zirconia

The porous textures of the two single-phase monoclinic zirconia samples studied were found to be relatively unstable; the specific surface areas and pore volumes were found to decrease markedly on increasing the calcination temperature (Fig. 1). The fact that neither of these samples underwent a phase change did not seem to have imparted any substantial stabilization against

sintering, even at the lower calcination temperatures. On the other hand, these monoclinic samples were more resistant to thermal sintering than were the predominantly tetragonal samples described in an earlier publication [2].

The loss of surface area and the decrease in the specific pore volume of monoclinic zirconia on calcination at increasing temperatures are both consistent with the extensive crystallite growth and agglomeration observed for these samples (Figs. 2 and 3). The process of crystallite growth is accompanied by the processes of inter-crystallite sintering, i.e. neck-formation and growth. The results of transmission electron microscopy showed that the fraction of the area of the crystallites which originates from the necks and which is thus not accessible (to nitrogen) increased steadily with increase in calcination temperature. In a previous publication [2], we showed that an estimate of the extent of inter-crystallite sintering can be obtained by comparing the specific surface area accessible to nitrogen (S_{BET}) with the corresponding geometrical specific surface area (S_{GEO}) calculated from the crystallite sizes, providing that there are no closed pores. Using geometric sintering models, we showed that the fraction of the geometrical area which is not accessible, i.e. $[(S_{GEO}-S_{BET})/S_{GEO}]$, can be directly correlated with the processes of agglomeration and/or neck-growth. In the latter case, $[(S_{GEO}-S_{BET})/S_{GEO}]$ is proportional to a parameter S_{NECK}/S_{GEO} on condition (i) that only one mass transport mechanism (i.e. sinter mechanism) is operative and (ii) that the interparticle coordination number is fixed; S_{NECK}/S_{GEO} represents the fraction (per interparticle contact) of the geometrical area which is neck-area. Fig. 7 shows how $[(S_{GEO}-S_{BET})/S_{GEO}]$ varies with calcination temperature for the sample RC100 (the filled circles); S_{GEO} was calculated from the data of Fig. 3 by assuming that the crystallites were spherical. This plot (Fig. 7) is in accordance with the TEM observations discussed above and shows that inter-crystallite sintering has a definite influence on the accessible surface areas and pore volumes of monoclinic zirconia; the fraction of the crystallite area which is not accessible increases steadily with increase in calcination temperature and is equal to 0.36 at the highest temperature. Considered altogether it must be concluded that crystallite growth, agglomeration (essentially an increase in the interparticle coordination number) as well as neck-formation and growth have an appreciable influence on the pore structure and surface area of monoclinic zirconia. As the highest calcination temperature is well below the Tamman temperature of zirconia (ca. 1200°C), the changes in the porous texture probably occur by a mechanism of surface diffusion. These conclusions are in good agreement with those reported by, for example, Rijnten [12], Crucean and Rand [14], Sharygin et al. [16], Mazdiyasni [47] and Veiga et al. [48].

Effect of additives on the development of the porous texture of monoclinic zirconia

Working on the principle that changes in the porous texture (occurring by a mechanism of surface diffusion) can be influenced by impregnation with

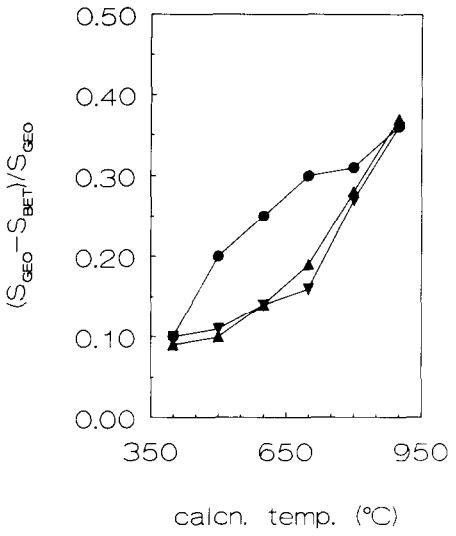

Fig. 7. The effect of lanthanum oxide on the processes of inter-crystallite sintering: (●) the sample RC100 (reference sample); (▲) the sample RC100-2.5La; and (▼) the sample RC100-2.7LaE.

suitable oxides [19,45,49,50], the effect of the addition of MgO, CaO, Y_2O_3 and La_2O_3 on the sintering of the monoclinic zirconia was studied. All the additives tested, apart from MgO, improved the thermal stability over the whole range of temperatures studied; MgO reduced the loss of surface area only at sinter temperatures up to 700°C (Fig. 4b). The best results were obtained with lanthanum oxide. At the lower calcination temperatures, i.e. up to 700°C, CaO and Y_2O_3 also performed well, yttria performing better than calcia. These results are in good agreement with the findings of Sauvion and Cailod [19] in that they also found that La_2O_3 was one of the most effective additives in preventing sintering in monoclinic zirconia; their results identified La_2O_3 as being better than SiO_2, Al_2O_3 or CeO_2.

A ranking $La_2O_3 > Y_2O_3 > CaO > MgO$ was determined for the effectiveness in stabilizing the porous texture of monoclinic zirconia up to 700°C (Fig. 4b). It is interesting to note that Tulier et al. [13], in studying the textural stabilization of non-porous metastable tetragonal zirconia at temperatures up to 650°C by the addition of lanthanum and yttrium oxide, found that yttria was superior to lanthana; 2 mol-% Y_2O_3 yielded almost the same effect as 4 mol-% La_2O_3. Since they found that both the textural and structural characteristics were stabilized by the addition of these dopants, they explained their results by suggesting that the changes occurring in the texture of zirconia are associated with phase transitions. Accordingly, the superiority of yttria to lanthana was explained by suggesting that Y_2O_3 was a better structural promoter for

tetragonal ZrO_2 than La_2O_3. (We have verified this particular argument experimentally). Furthermore, these results are in good agreement with our own suggestion [2] that the changes in the porous texture of tetragonal zirconia are associated with the transport of material (by surface diffusion), a process which is accelerated by the phase transition of tetragonal to monoclinic. On the other hand, the results obtained in the present study regarding monoclinic zirconia calcined at temperatures up to 700°C suggest that when there is little to no phase transformation, lanthanum oxide is more effective in suppressing the transport of mass by surface diffusion than is yttrium oxide. Thus, the results obtained in this investigation and those of Turlier et al. can be regarded as being complementary, for they show that the crystallographic structure of the zirconia support material determines the relative effectiveness of the additives and hence also the choice of the most suitable additive.

The behaviour of the doped samples at calcination temperatures above about 700°C is characterized by the following features: (i) the effectiveness of lanthana, yttria and calcia as a sintering inhibitor for 'monoclinic' zirconia was found to decrease markedly with increase in calcination temperature (Figs. 4b and 6b); (ii) whereas yttria performed better than calcia at calcination temperatures lower than approximately 850°C, the reverse was found to be true at temperatures in excess of 850°C (Fig. 4b); and (iii) at temperatures above 700°C, MgO was found to have a detrimental effect on the surface area of zirconia (Fig. 4). These observations can all be accounted for on the basis of the XRD results, particularly those of the phase analyses.

It is conceivable that a textural promoter can preserve its effectiveness in preventing sintering controlled by surface diffusion only if it remains on the surface of the substrate in a well-dispersed and stable state (either as a single oxide or as a distinct surface phase). Diffusion into the bulk of the substrate (forming solid solutions and/or inducing extensive phase transitions), coagulation to form crystallites of its own preferred phase (which can grow further by heating at higher temperatures), or 'dewetting' and agglomeration into ordered phases will only lead to a decrease in the effectiveness of stabilization. According to the phase diagrams for ZrO_2 with MgO [51,52] and La_2O_3 [53], there is very little solubility of either of these two additives in monoclinic zirconia, the solubility of both oxides being at the most about 0.5 mol-% at temperatures below 1000°C. Calcium and yttrium oxide, on the other hand, dissolve to a significant extent in monoclinic zirconia. According to Stubican and coworkers [52,54,55], the solubility of CaO in monoclinic zirconia at low temperatures (below 1000°C) is no more than 3 mol-% but the solubility is already significant at temperatures above about 500°C. The maximum solubility of Y_2O_3 in monoclinic zirconia is reported to be approximately 1.5 mol-%, this being reached at a temperature of about 500°C [52,56–58]. Besides these aspects of solubility, all the additives investigated are able to form (metastable) fluorite-type phases with zirconia; hence, phase transitions are likely to be

induced when and if these are incorporated in sufficiently high concentrations into the zirconia matrix. The occurrence of an appreciable phase transformation is particularly detrimental to the stability of the texture of zirconia for, as discussed in the preceeding paragraphs, it is likely to bring about a substantial increase in the mobility of the solid phase and thus in the rate of sintering. What is more, according to the phase equilibria of ZrO_2 with CaO and Y_2O_3, the solubility of these two additives in the fluorite-like modification is greater than in the monoclinic one.

The phase transitions observed in this study for the CaO- and Y_2O_3-doped samples (Fig. 5) are in agreement with the respective binary phase equilibria, with the understanding that the fluorite-like phase is metastable in both cases; the fluorite-like phase can be regarded as being an intermediate step on the way to the ordered phases $CaZrO_3$ and $Zr_3Y_4O_{12}$. In view of the considerations outlined in the previous paragraph, the decrease in the effectiveness of CaO and Y_2O_3 as sintering inhibitors is believed to be associated primarily with the extensive diffusion of these cations into the bulk of the zirconia crystallites and the subsequent phase transition to the metastable fluorite-like modification. Accordingly, the observed inversion of the order of effectiveness after calcination above about 850°C (Fig. 4) is ascribed to the greater extent of phase transformation in the case of yttria as compared to calcia.

The rationalization of the influence of MgO is of necessity different. The results of the phase analyses obtained for the MgO-doped samples are in good agreement with the most recent phase diagrams published for the system ZrO_2–MgO [51,55,59]; these show that monoclinic zirconia and MgO coexist as separate phases over the entire range of compositions up to 50 mol-% MgO at temperatures below approximately 1070°C. Although MgO does not seem to interact to a great extent with monoclinic zirconia, we have found that it slows down the growth of the monoclinic crystallites at calcination temperatures up to 800°C; the effectiveness hereof, however, was found to decrease markedly on increasing the calcination temperature and after heat treatment at 900°C there was no significant difference in size between the zirconia crystallites of the MgO-doped sample and of the reference sample. To account for the experimental data regarding MgO, the following model is proposed: after impregnation and calcination at 400°C, MgO is present in a well-dispersed or amorphous state, thus giving rise to an increased resistance to thermal sintering [the stabilizing effect of MgO is initially (400–500°C) comparable with that of the other three oxides (Fig. 4b)]. Upon calcination at higher temperatures, coagulation and/or crystal growth of the MgO occurs, leading to a decrease in the effective surface coverage by MgO and consequently to a decrease in the stabilizing effect; after sintering at 900°C, the MgO crystallites are large enough to be detectable by XRD. In accordance with this rationalization, the destabilization of the texture of monoclinic zirconia after calcination at temperatures in excess of 700°C (Fig. 4) can be explained by assuming that the MgO

crystallites are located at the junctions of the monoclinic zirconia crystallites which make up the agglomerates. In other words, the detrimental effect of MgO on the texture is believed to be largely due to a physical blocking of the surface of the monoclinic crystallites by MgO crystallites.

Since the extent of the phase transformation in the case of the La_2O_3-doped samples is not very extensive (see e.g. Fig. 5), the decrease in the effectiveness of this additive as a sintering inhibitor at calcination temperatures in excess of 700 °C cannot be brought about (solely) by this process. As discussed in the preceeding subsection, sintering controlled by surface diffusion manifests itself macroscopically through the occurrence of the processes of crystallite growth and inter-crystallite sintering. The effect of lanthanum oxide on these two processes is illustrated in the Figs. 7, 8 and 9 using the results obtained for the samples promoted with approximately one-fourth of a theoretical monolayer quantity of $LaO_{1.5}$ (RC100-2.5La and RC100-2.7LaE); Fig. 7 shows the influence of lanthana on the processes of inter-crystallite sintering; Fig. 8 shows representative TEM micrographs of selected calcined samples (all the micrographs are shown at the same magnification as those presented in Fig. 2); and Fig. 9 summarizes the results of the X-ray line-broadening analyses (the values are in excellent agreement with the TEM results). It is clear from the Figs. 8 and 9 that the growth of the monoclinic crystallites upon calcination in static air is strongly inhibited by the addition of lanthana. From the variation of $[(S_{GEO}-S_{BET})/S_{GEO}]$ with calcination temperature (Fig. 7) it can also readily be inferred that the processes of agglomeration and neck-formation and growth are significantly hindered up to 700 °C by the addition of La_2O_3. Above 700 °C, the fraction $[(S_{GEO}-S_{BET})/S_{GEO}]$ is seen to increase markedly with increase in calcination temperature. (Note that these results are verified by the TEM results). The increase in the contribution of the processes of inter-crystallite sintering and thus also of the process of crystallite growth to the overall process of surface area loss, was shown (by XRD) to coincide with the appearance of the pyrochlore compound $Zr_2La_2O_7$. To account for all of the experimental data regarding La_2O_3, the following model is proposed: regardless of the lanthanum oxide concentration employed (up to 8.0 mol-% $LaO_{1.5}$), lanthana is initially present in a highly dispersed or amorphous state (i.e. not detectable by XRD); this situation prevails up to a calcination temperature of about 700 °C. This lanthanum oxide considerably improves the thermal stability of monoclinic zirconia by strongly inhibiting the processes of crystallite growth and inter-crystallite sintering (agglomeration as well as neck-formation and growth) and thus the process of mass transport by surface diffusion. On calcination at higher temperatures (> 700 °C), 'dewetting' and agglomeration into X-ray detectable lanthanum zirconate crystallites occurs; this leads to a decrease in the effective surface coverage by lanthana and consequently to a decrease in the stabilizing effect. This process is most probably aided by the simultaneous occurrence of the phase transition from monoclinic to sta-

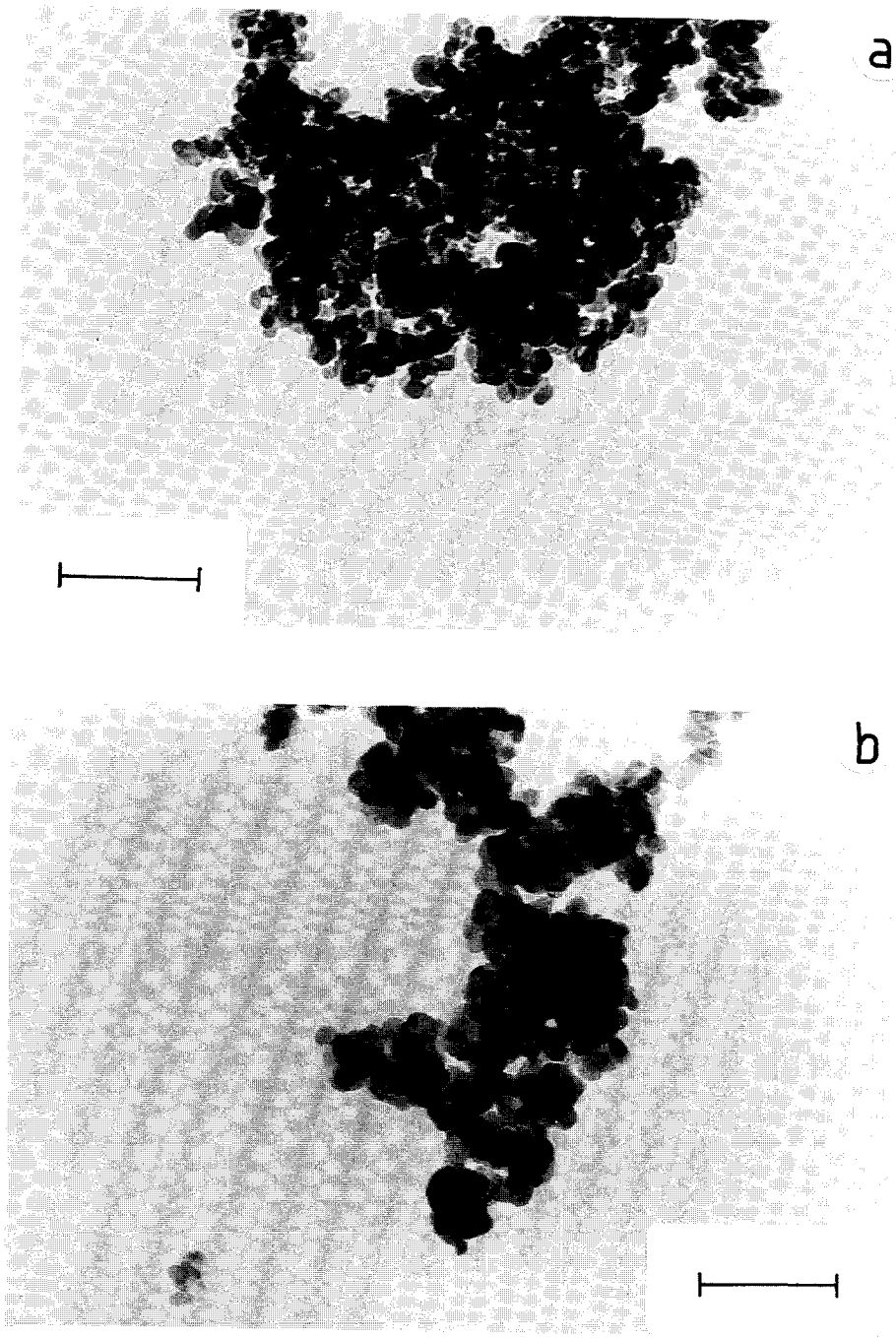

Fig. 8. Transmission electron micrographs of the sample RC100-2.5La calcined at (a) 500 °C, (b) 700 °C and (c) 900 °C, and of the sample RC100-2.7LaE calcined at (d) 700 °C and (e) 900 °C. The bar indicates a measurement of 100 nm.

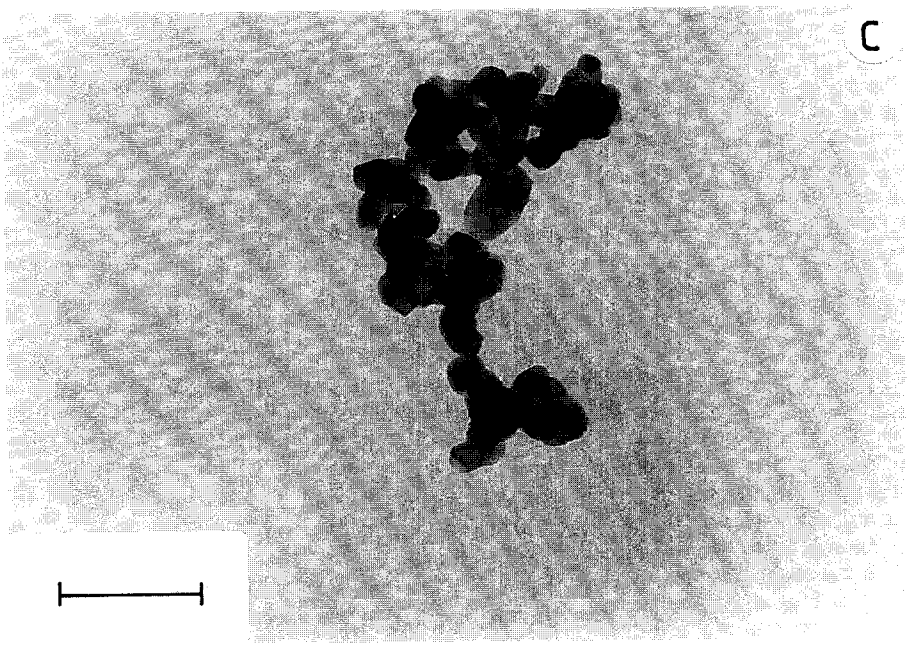
c

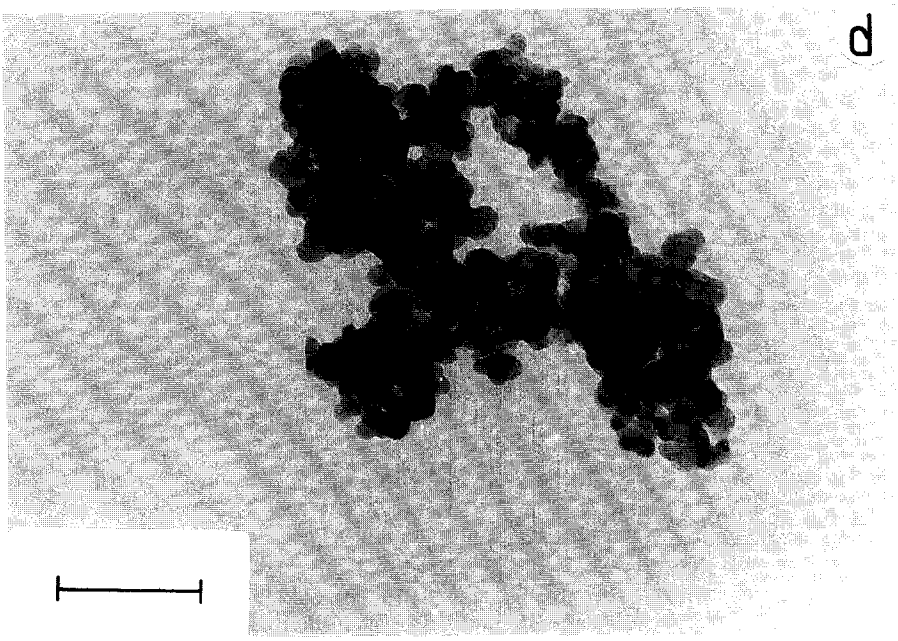
d

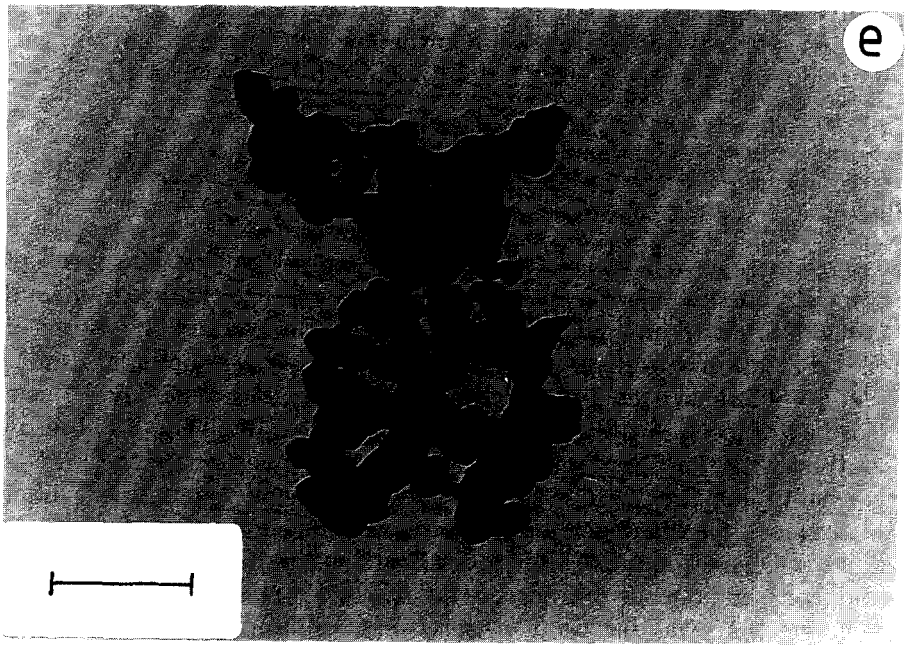

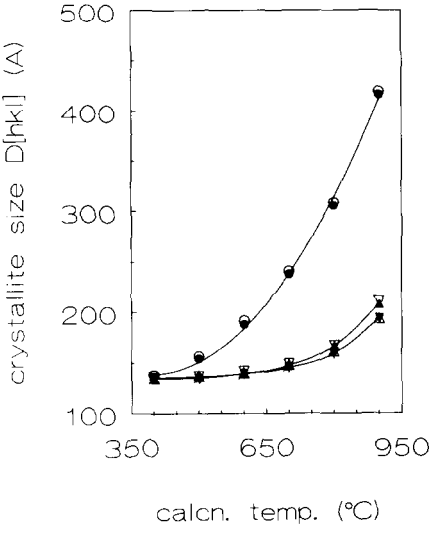

Fig. 9. The effect of lanthanum oxide on the process of crystallite growth in monoclinic zirconia: (● and ○) RC100 (reference sample); (▲ and ▽) RC100-2.5La; (▼ and △) RC100-2.7LaE; filled symbols: the size calculated using the (11 – 1) reflection of the monoclinic phase; open symbols: the size calculated using the (111) reflection of the monoclinic phase.

bilized tetragonal zirconia. [It should be noted that this model also explains the observation that the effectiveness of lanthana addition, particularly at calcination temperatures above 700°C, does not reach a plateau at 8.0 mol-% $LaO_{1.5}$ (Fig. 6b).]

Influence of the impregnation procedure on the thermal stability of monoclinic zirconia

Two procedures have been used to apply lanthanum oxide to the surface of monoclinic zirconia: (i) impregnation with a lanthanum nitrate solution; and (ii) impregnation with an aqueous solution of $[La(EDTA)]^-$. The degree of textural stabilization obtained with these two procedures was similar at similar surface concentrations (see Tables 5 and 6), the use of $[La(EDTA)]^-$ as a precursor having no significant advantage over that of $La(NO_3)_3$. These results contrast with the findings of Tijburg [37] who investigated the La_2O_3/γ-Al_2O_3 system and found that the amount of lanthana required to render γ-Al_2O_3 thermostable was dependant on the method of application, the adsorption of a La(EDTA)-complex being more effective than incipient wetness impregnation with an aqueous solution of $[La(EDTA)]^-$; the latter method was more effective than was incipient wetness impregnation with a solution of $La(NO_3)_3$. Tijburg rationalized his results in terms of the state of dispersion of the applied lanthanum oxide, specific adsorption yielding the highest dispersions. To account for our results, we suggest that similar dispersions are obtained after calcination in static air whether impregnation is carried out with an aqueous solution of $[La(EDTA)]^-$ or of $La(NO_3)_3$; this applies for surface coverages up to at least approximately half a monolayer. Thus, as distinct from the system La_2O_3/γ-Al_3O_3, the extent of the interaction between the lanthanum complex and the zirconia surface is believed to be comparable to that between La^{3+}/NO_3^- and zirconia.

CONCLUSIONS

1. Single-phase monoclinic zirconia with a high specific surface area and without any microporosity can be made by means of gel-precipitation.

2. Notwithstanding the fact that it is structurally stable, the thermal stability of monoclinic zirconia was not satisfactory under the experimental conditions employed; the high initial specific surface area and pore volume were lost quite rapidly with increase in calcination temperature.

3. The thermal stability of monoclinic zirconia was considerably improved by the addition of inorganic oxides such as CaO, Y_2O_3 and La_2O_3; these additives were effective over the entire range of temperatures studied, 400 to 900°C. The addition of MgO resulted in an improvement in the thermal stability only at calcination temperatures up to 700°C.

4. Lanthanum oxide was found to be the most effective additive for improv-

ing the thermal stability of monoclinic zirconia. The effectiveness of lanthana addition did not reach a plateau at 8.0 mol-% $LaO_{1.5}$. However, modification with an amount equivalent to 20–50% of the theoretical monolayer quantity of $LaO_{1.5}$ would suffice to ensure that a monoclinic zirconia material has sufficiently high thermal stability for practical applications (e.g. in the use of monoclinic zirconia as a catalyst support).

5. Up to a calcination temperature of 700°C, a ranking $La_2O_3 > Y_2O_3 > CaO > MgO$ was determined for the effectiveness in stabilizing the porous texture of monoclinic zirconia. The parameters determining this ranking were: (i) the solubility of the dopant in (monoclinic) zirconia; (ii) the extent of the interaction between the textural promoter and the substrate; and (iii) the crystallographic structure of the zirconia support material itself, in which the occurrence of appreciable phase transformations must be limited.

6. The same effect on the thermal stability of monoclinic zirconia was obtained whether impregnation was carried out with an aqueous solution of the poorly-crystallizing complex $[La(EDTA)]^-$ or of $La(NO_3)_3$.

7. The influence of the presence of additives as well as that of the calcination temperature on the evolution of the porous texture of the monoclinic zirconia could be accounted for by a model involving mass transport by a surface diffusion mechanism.

ACKNOWLEDGEMENTS

The authors should like to thank H. Weber for performing the chemical analyses and J. Boeijsma for his assistance with the X-ray diffraction measurements. Thanks are also due to Dr. C. Otto, from the Faculty of Applied Physics, for his assistance in recording the laser Raman spectra and to Dr. J. Beyer, from the Faculty of Mechanical Engineering, for carrying out the TEM-experiments. This research was partially financed by the Dutch Ministry of Economic Affairs (Innovative Research Program on Catalysis).

REFERENCES

1 K. Tanabe, Mater. Chem. Phys., 13 (1985) 347.
2 P.D.L. Mercera, J.G. van Ommen, E.B.M. Doesburg, A.J. Burggraaf and J.R.H. Ross, Appl. Catal., 57 (1990) 127.
3 H. Fujii, N. Mizuno and M. Misono, Chem. Lett., (1987) 2147.
4 L.A. Bruce and J.F. Mathews, Appl. Catal., 4 (1982) 353.
5 L.A. Bruce, G.J. Hope and J.F. Mathews, Appl. Catal., 8 (1983) 349.
6 P. Turlier, H. Praliaud, P. Moral, G.A. Martin and J.A. Dalmon, Appl. Catal., 19 (1985) 287.
7 G.R. Gavalas, C. Phichitkul and G.E. Voecks, J. Catal., 88 (1984) 54.
8 K.E. Smith, R. Kershaw, K. Dwight and A. Wold, Mater. Res. Bull., 22 (1987) 1125.
9 S. Narayanan and G. Sreekanth, J. Chem. Soc., Faraday Trans., 1, 85 (1989) 3785.
10 P. Marginean and A. Olariu, J. Catal., 95 (1985) 1.

11 E.C. Subbarao, in A.H. Heuer and L.W. Hobbs (Editors), Science and Technology of Zirconia, Adv. Ceram., 3 (1981) 1.
12 H.Th. Rijnten, Thesis, Delft University of Technology, 1971.
13 P. Turlier, J.A. Dalmon, G.A. Martin and P. Vergnon, Appl. Catal., 29 (1987) 305.
14 E. Crucean and B. Rand, Trans. J. Brit. Ceram. Soc., 78 (1979) 58.
15 M. Valigi and D. Gazzoli, in P. Barret and L.-C. Dufour (Editors), Reactivity of Solids, Proc. 10th Int. Symp. Reactivity of Solids, Dijon, Mater. Sci. Monogr., 28B (1985) 1081.
16 L.M. Sharygin, V.M. Galkin and S.P. Kurushin, Kinet. Catal. (English Trans.), 16 (1975) 1382.
17 T. Yamaguchi and K. Tanabe, Mater. Chem. Phys., 16 (1986) 67.
18 R. Srinivasan, M.B. Harris, S.F. Simpson, R.J. De Angelis and B.H. Davis, J. Mater. Res., 3 (1988) 787.
19 G.-N. Sauvion and J. Cailod, French Pat. Appl. FR 2590887-A1 (1987).
20 K.S. Mazdiyasni, Ceram. Int., 8 (1982) 42.
21 B.E. Yoldas, J. Mater. Sci., 21 (1986) 1080.
22 M. Bensitel, O. Saur and J.C. Lavalley, Mater. Chem. Phys., 17 (1987) 249.
23 H. Nishizawa, N. Yamasaki and K. Matsuoka, J. Am. Ceram. Soc., 65 (1982) 343.
24 E. Tani, M. Yoshimura and S. Somiya, J. Am. Ceram. Soc., 64 (1981) C-181.
25 A.T. Liu and P. Kleinschmit, in R.W. Davidge (Editor), Novel Ceramic Fabrication Processes and Applications, Proc. Brit. Ceram. Soc., 38 (1986) 1.
26 Y. Murase and E. Kato, Nippon Kagaku Kaishi, 3 (1978) 367.
27 A. Clearfield, Inorg. Chem., 3 (1964) 146.
28 Y. Murase and E. Kato, J. Am. Ceram. Soc., 66 (1983) 196.
29 K. Haberko, Ceramurgia Int., 5 (1979) 148.
30 S.L. Jones and C.J. Norman, J. Am. Ceram. Soc., 71 (1988) C-190.
31 M.S. Kaliszewski and A.H. Heuer, J. Am. Ceram. Soc., 73 (1990) 1504.
32 T. Kosmac, R. Gopala Krishnan, V. Krasevec and M. Komac, J. Physique Colloque C1, 47 (1986) C1-43.
33 P.D.L. Mercera, J.G. van Ommen, E.B.M. Doesburg, A.J. Burggraaf and J.R.H. Ross, in preparation.
34 M.A.C.G. van de Graaf, J.H.H. ter Maat and A.J. Burggraaf, J. Mater. Sci., 20 (1985) 1407.
35 R.D. Shannon, Acta Cryst., A32 (1976) 751.
36 G.R. Meima, Thesis, State University of Utrecht, 1987.
37 I.I.M. Tijburg, Thesis, State University of Utrecht, 1989.
38 H. Toraya, M. Yoshimura and S. Somiya, J. Am. Ceram. Soc., 67 (1984) C-119.
39 S.J. Gregg and K.S.W. Sing, Adsorption, Surface Area and Porosity, 2nd edn., Academic Press, London, 1982.
40 K.S.W. Sing, D.H. Everett, R.A.W. Haul, L. Moscou, R.A. Pierotti, J. Rouquerol and T. Siemieniewska, Pure Appl. Chem., 57 (1985) 603.
41 B.C. Lippens and J.H. de Boer, J. Catal., 4 (1965) 319.
42 J.D. McCullough and K.N. Trueblood, Acta Cryst., 12 (1959) 507.
43 K.C. Pratt, J.V. Sanders and V. Christov, J. Catal., 124 (1990) 416.
44 M. Bettman, R.E. Chase, K. Otto and W.H. Weber, J. Catal., 117 (1989) 447.
45 H. Schaper, Thesis, Delft University of Technology, 1984.
46 T. Machej, P. Ruiz and B. Delmon, J. Chem. Soc., Faraday Trans., 86 (1990) 731.
47 K.S. Mazdiyasni, in J.W. Mitchell, R.C. de Vries, R.W. Roberts and P. Cannon (Editors), Reactivity of Solids, Wiley Interscience, New York, 1969, p. 115.
48 M.L. Veiga, M. Vallet, A. Jerez and C. Pico, Ann. Chim. Fr., 6 (1981) 345.
49 P. Burtin, J.P. Brunelle, M. Pijolat and M. Soustelle, Appl. Catal., 34 (1987) 225.
50 C. Xu, J. Tamaki, N. Miura and N. Yamazoe, J. Mater. Sci. Lett., 8 (1989) 1092.
51 S.M. Sim and V.S. Stubican, J. Am. Ceram. Soc., 70 (1987) 521.

52 V.S. Stubican, in S. Somiya, N. Yamamoto and H. Yanagida (Editors), Science and Technology of Zirconia III, Adv. Ceram., 24 (1988) 71.
53 B. Bastide, P. Odier and J.P. Coutures, J. Am. Ceram. Soc., 71 (1988) 449.
54 V.S. Stubican and S.P. Ray, J. Am. Ceram. Soc., 60 (1977) 534.
55 J.R. Hellmann and V.S. Stubican, J. Am. Ceram. Soc., 66 (1983) 260.
56 H.G. Scott, J. Mater. Sci., 10 (1975) 1527.
57 C. Pascual and P. Duran, J. Am. Ceram. Soc., 66 (1983) 23.
58 R. Ruh, K.S. Mazdiyasni, P.G. Valentine and H.O. Bielstein, J. Am. Ceram. Soc., 67 (1984) C-190.
59 V.S. Stubican and J.R. Hellmann, in A.H. Heuer and L.W. Hobbs (Editors), Science and Technology of Zirconia, Adv. Ceram., 3 (1981) 25.